MODELLING OF POTENTIAL UNDERWATER NOISE FROM PILE DRIVING AT THE TOWNSVILLE OCEAN TERMINAL

Report 2

Version 1.0

Prepared by:

Isabelle Gaboury
Chris Levy
Dr. Christine Erbe
55 Fiddlewood Crescent
Bellbowrie, Qld 4070
T: 07-3202 9883
Email: Christine@jasco.com

Prepared for:

Simon Mustoe
AES Applied Ecology Solutions Pty Ltd
39 The Crescent
Belgrave Heights, Vic3160
Tel: +61 (0) 3 97526398
Mob: +61 (0) 40522083
Email: simonmustoe@ecology-solutions.com.au

Brisbane, 16 July 2008

Table of Contents

List of Figures

List of Tables

1 Project Description

As part of the integrated Townsville Ocean Terminal Project (TOT), about 200m worth of sheet piles are proposed to be driven into the ground near the existing breakwaters of Townsville Harbour.

Figure 1: Satellite image of Townsville Harbour showing the existing Western and Northern Breakwater.

The proposed section of sheet piling is indicated in the following figure.

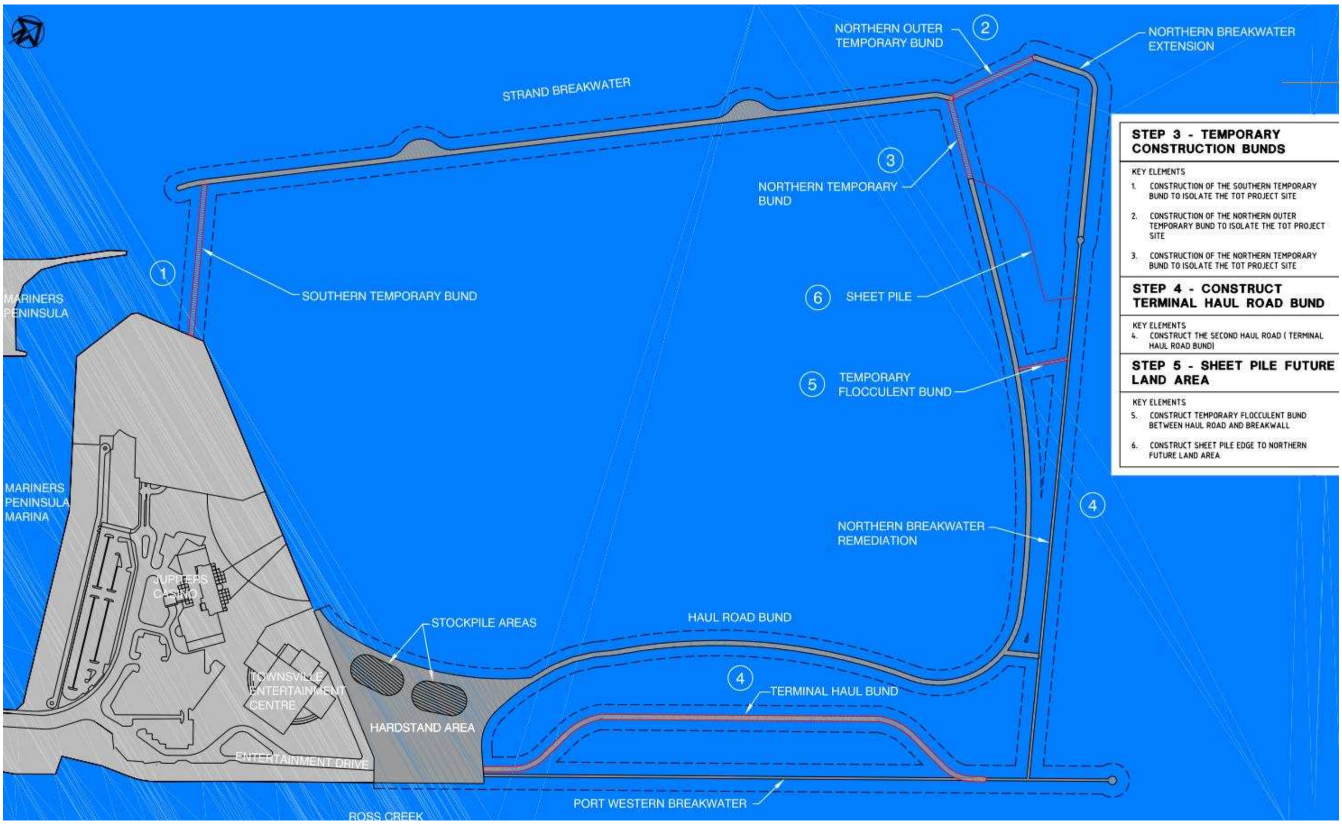

Figure 2: Bund and breakwater construction map, indicating the proposed section of sheet piles as a thin red line. The total length of sheet piling is about 200m.

The sheet piles are going to be made of steel. They will be either U or Z shaped, about 1m wide and 15m long. The sheet thickness will be approximately 2cm. The sheets will interlock. A total of about 200 sheet piles will be driven.

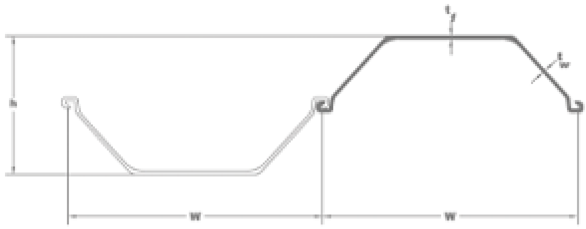

Figure 3: Sketch of the sheet piles possibly used at the TOT.

JASCO Research Ltd has been contracted to provide an assessment of potential underwater sound emissions during pile driving operations.

2 The Acoustics of Pile Driving

Numerous studies on underwater noise emission during marine construction have identified pile driving as the loudest source (e.g. Greene *et al.* 2008, Moulton *et al.* 2003). One can distinguish between two general methods of driving piles: vibratory piling and impact piling.

Vibratory pile drivers contain a system of counter-rotating eccentric weights, arranged such that horizontal vibrations cancel out while vertical vibrations get transmitted into the pile. The vibratory pile driver is lifted and positioned over the pile, and gradually moves the pile into the ground. Vibratory piling is used when the substrate is relatively soft. The sound from vibratory pile driving is continuous. Noise emission is less compared to impact piling. At this stage, sheet piles for the TOT Project are planned to be driven with a vibratory driver through the top layers of sediment. A switch to impact driving will be made if and when the piles hit highly compressed or dense substrate.

During impact piling, a heavy weight hammers the pile into the ground. There are different methods for lifting the weight, including hydraulics, steam or diesel. In the case of diesel hammering, the weight is initially raised by auxiliary means, e.g. a crane, which draws air into the cylindrical housing of the hammer or piston. The weight is then released and falls by gravity onto the top of the pile to be driven. The weight compresses the air in the cylindrical housing, heating it to the ignition point of diesel fuel injected into the cylinder. The fuel-air mixture detonates, transferring the energy of the falling weight to the pile head and driving the weight back up. The rising weight draws in more fuel-air mixture, and the cycle starts again.

Impact piling is louder in air and under water than vibratory piling. When the hammer strikes the pile (and also when the fuel detonates in the case of a diesel hammer), sound is created in air at the top of the pile. Acoustic energy spreads as a spherical wave through the air. The impact also gives rise to a stress wave travelling down the length of the pile. This wave couples with the surrounding medium (first air, further down water), radiating acoustic energy into the air and water. The stress wave in the pile also couples with the substrate below the water, creating an acoustic wave travelling through the seafloor. Sound can travel very fast and with low attenuation through certain types of seafloor. At some distance away from the pile, acoustic energy can radiate back into the water column from the seafloor. The sound from impact pile driving is transient and discontinuous, called pulsed. Within the water column, the arrival of acoustic pulses from different media and directions and with different phases and time delays tends to result in a complex pattern of louder and quieter regions, in particular close to the source.

The level of noise received in the water column at some distance from the pile depends on a multitude of factors, including the size, shape, length and material of the pile, the size and energy of the hammer, the type of sediment and the thickness of the sediment, the type and depth of the underlying bedrock, the water depth, bathymetry, salinity and temperature.

It is impossible to accurately predict the level of noise emission from pile driving prior to the commencement of operations. For the current TOT noise assessment, we have reviewed the literature on pile driving, and we have taken measurements from other studies to model sound propagation near Townsville Harbour.

2.1 Sound Metrics

2.1.1 Peak Pressure

Hydrophones are essentially pressure sensors. If *p(t)* is the time series of pressure measured in the water column, then the peak sound pressure level (also sometimes called 0-peak sound pressure level) is the maximum absolute value of the overpressure for an impulsive event like impact pile driving. It is not an average, but the largest positive value during a specified time:

$$SPL_{Pk} = 20\log_{10}\left(\max(p(t))\right)$$

This quantity is measured in dB re 1µPa.[1]

The peak-to-peak sound pressure level [dB re 1 µPa] is the difference between the maximum and minimum overpressures of a time series of an impulsive event:

$$SPL_{Pk-Pk} = 20\log_{10}\left(\max(p(t)) - \min(p(t))\right)$$

2.1.2 RMS Pressure

The root-mean-square (rms) pressure [dB re 1 µPa] is one of the standard metrics for continuous sound as from vibratory pile driving or ambient noise. In the case of impulsive sound as from impact pile driving, the rms value is calculated over the duration of the pulse. The duration of a pulse is defined as the time over which 90% of the total energy is received. On a cumulative energy curve, the start-time of a pulse is taken at the 5% cumulative energy mark, and the end-time of a pulse is taken at the 95% cumulative energy mark. The rms value requires integration of the squared pressure time series and division by the total length T of the signal:

$$SPL_{rms} = 20\log_{10}\left(\sqrt{\frac{1}{T_{90}}\int_{T_{90}} p(t)^2\,dt}\right)$$

The subscript 90 indicates that the duration of the signal corresponds to 90% of total energy in the case of pulsive events. For continuous signals, the subscript is dropped.

2.1.3 Sound Exposure Level

The sound exposure level corresponds to the total energy of a signal. It is measured in dB re 1 µPa^2·s:

$$SEL = 10\log_{10}\left(\int_T p(t)^2\,dt\right)$$

2.1.4 1/3 Octave Band Levels

Underwater noise is commonly plotted in 1/3 octave band levels. From one octave to the next, frequency doubles. 1/3 octaves split each octave into three adjacent bands, not linearly but logarithmically. The centre frequencies *fc* of the adjacent 1/3 octave bands used in the following analysis are in Hz:

10, 13, 16, 20, 25, 32, 40, 50, 63, 80, 100, 126, 160, 200, 251, 320, 400, 500, 640, 800, 1000, 1280, 1585, 2000, 2560, 3162, 4000, 5000, 6310, 8000

The width of each 1/3 octave band can be computed as the difference between the upper and the lower cut-off frequencies. The lower cut-off frequency is $2^{-1/6} * fc$; the upper cut-off frequency is $2^{1/6} * fc$. As *fc* increases, the bands become wider and wider. While this might seem mathematically confusing, this logarithmic convention is based on human hearing.

If one filters the sound recording by a series of adjacent 1/3 octave band filters, one can compute sound pressure levels and sound exposure levels for each 1/3 octave band. These are then referred to as 1/3 octave band levels. Conceptually, 1/3 octave band levels give the total pressure or the total energy in each band.

2.1.5 Power Spectrum Density Levels

1/3 octave band levels are often computed from power spectrum densities. Power

[1] Underwater the reference pressure is 1µPa. In air, the standard reference pressure is 20µPa.

spectrum density levels give the squared sound pressure in a series of adjacent bands of a constant 1 Hz width. They could thus be called 1Hz band levels, but have historically been referred to as power spectrum density (PSD) levels in dB re 1µPa^2/Hz.

2.2 Pile Driving Source Levels

In our previous report on TOT underwater acoustics (JASCO 2008), we reviewed the literature on pile driving noise. Unfortunately only a handful of reports published sound spectra, i.e. sound levels as a function of frequency. In Blackwell *et al.* (2004), levels were very quiet, because piles were driven into a gravel island, rather than into the seafloor at some depth below the water surface. These data are therefore not used for the TOT model. Caltrans (2001) and Greeneridge (1999) published usable spectrum levels. We augmented these data with three data sets collected by ourselves and colleagues in shallow water. Nehls *et al.* (2007) published pile driving spectra in units of sound exposure level. Unfortunately, no source levels, pressure levels or pulse durations were given, making it difficult to use these measurements for a sound propagation model. In general, however, the data fall into the range of the other studies.

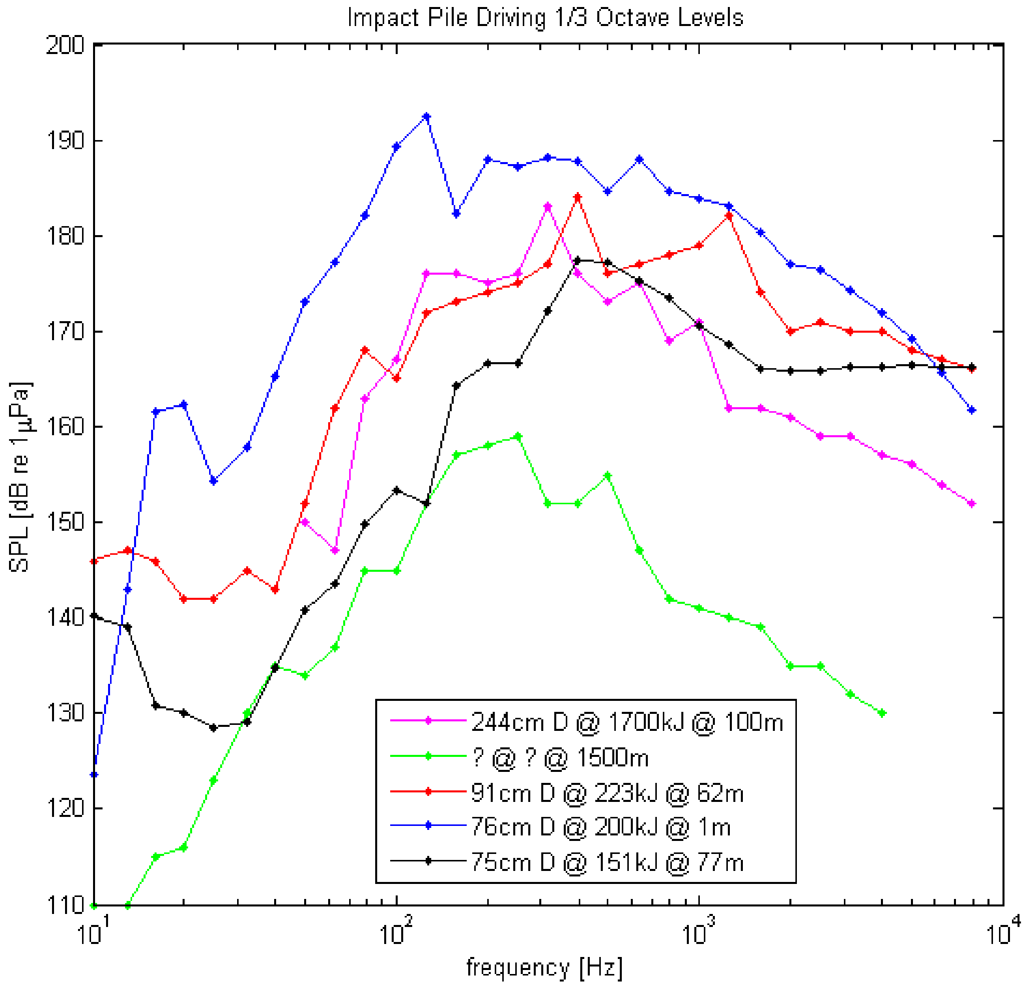

Figure 4: Pile driving spectra from five different studies, given as 1/3 octave band levels. Pink: from Caltrans 2001; green: from Greeneridge 1999; red, blue, black: by JASCO & colleagues (classified). The legend gives the pile diameter in cm, the maximum energy of the hammer in kJ and the range at which the measurements were taken in m. Greeneridge did not report the pile size nor the hammer energy.

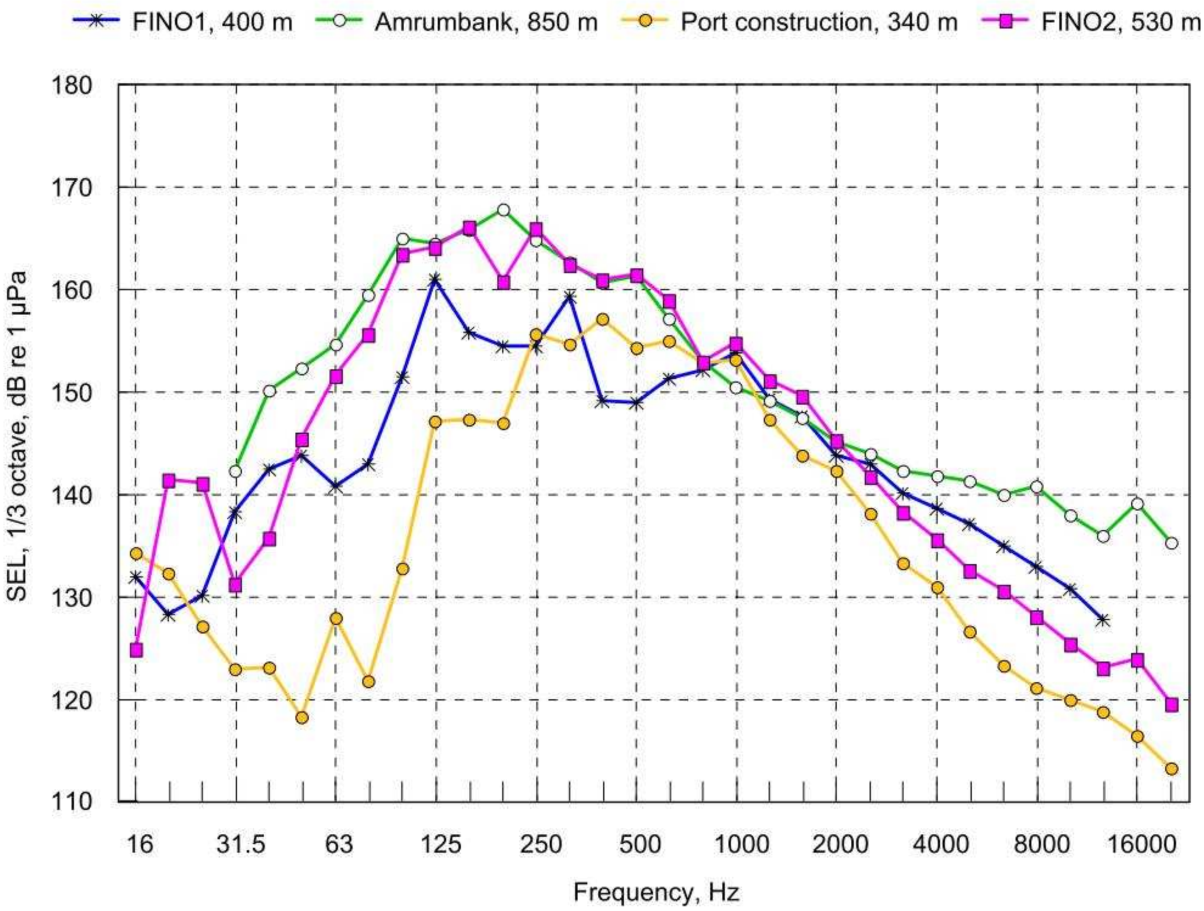

Figure 5: Pile driving recordings reviewed by Nehls *et al.* (2007) and reprinted for comparison. Unfortunately, no source levels or pulse durations or propagation characteristics were listed, making it impossible to use these data for the TOT model. In general, however, these levels fit in with the above measurements.

To estimate source levels, we used the measurements by Caltrans (2001) and Greeneridge (1999) and our own, and applied a cylindrical spreading loss model. All measurements were taken in very shallow water, where sound will mostly spread cylindrically. With *RL* being the received level at some range *R*, and *SL* being the source level at 1m, the latter was estimated according to

$$SL = RL + 10*\log10(R) \quad .$$

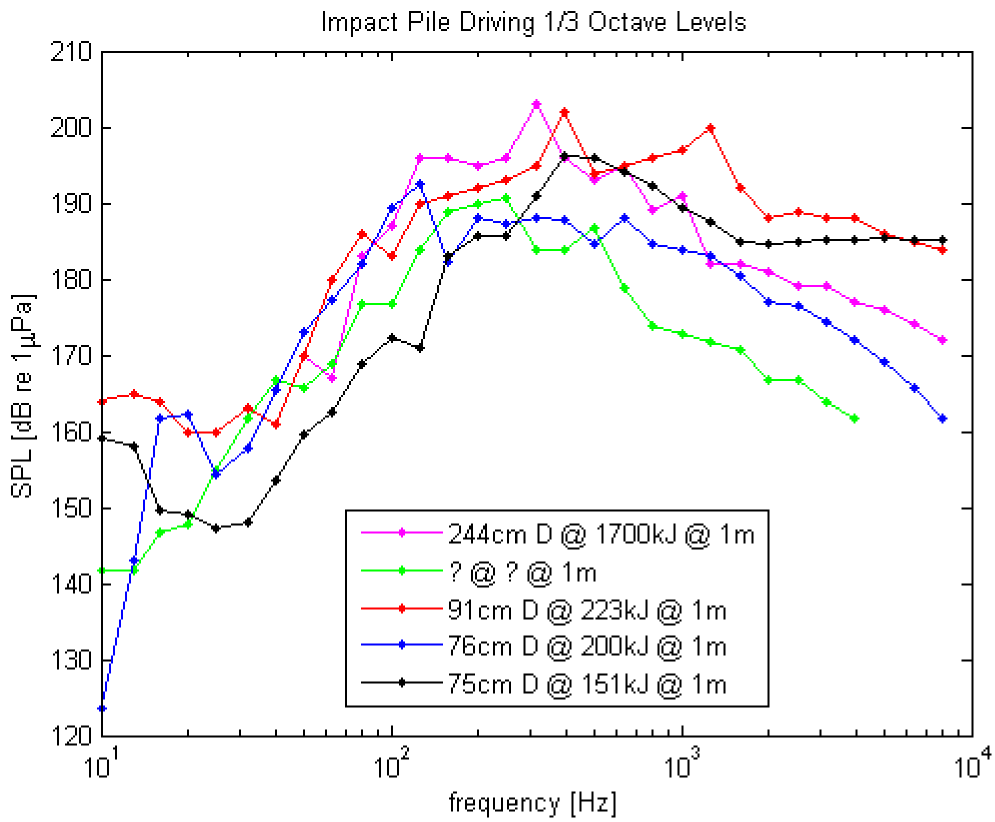

Figure 6: Source spectra in 1/3 octave band levels, all referenced to 1m after applying a cylindrical spreading loss model.

For the TOT model, we used the envelope of these spectra, i.e. the maximum and minimum at each frequency. The top black line in the following figure is used to model a 'loud' source; the lower black line is used to model a 'quiet' source.

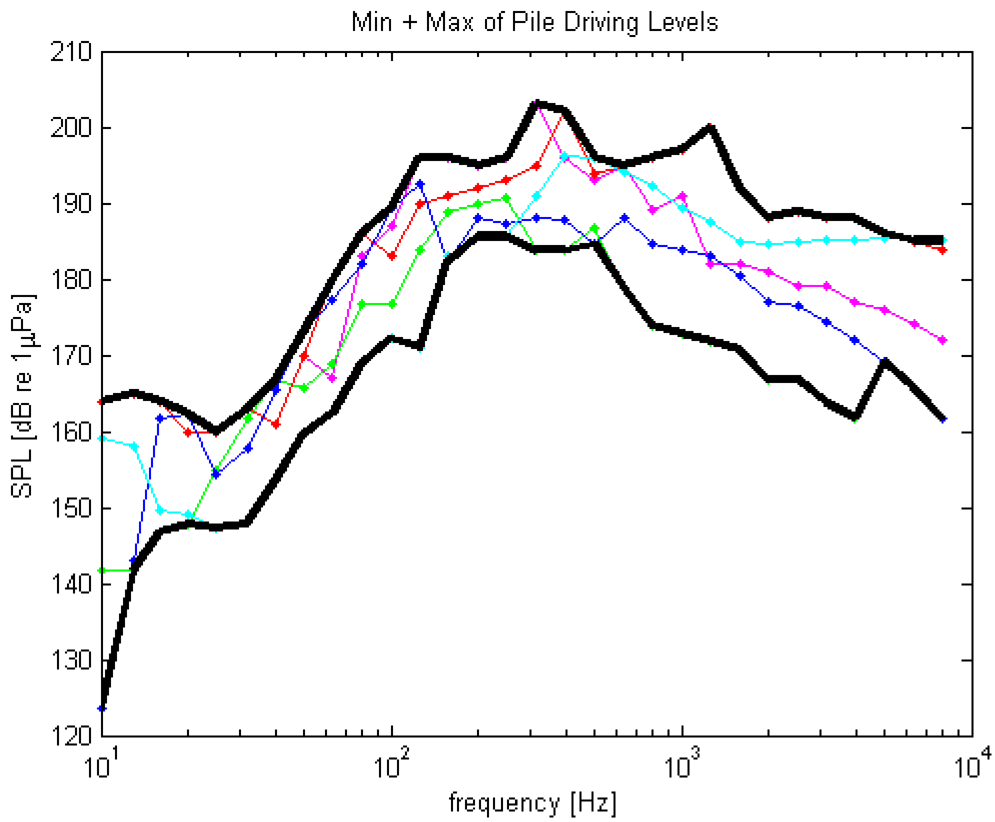

Figure 7: Envelope of pile driving source spectra, which was used for the TOT model.

3 Modelling Sound Propagation

This section describes how acoustic energy spreads away from the source and through the marine environment. JASCO has developed a variety of sound propagation models, which excel in different environments. To model sound propagation at the TOT site, we use our Marine Operations Noise Model (MONM).

3.1 Model Details

MONM is a proprietary application developed by JASCO Research. It is an advanced modelling package whose algorithmic engine is a modified version of the widely-used Range-dependent Acoustic Model (RAM) and its companion code RAMS (Collins *et al.* 1996).

RAM and RAMS are based on the parabolic equation method using the split-step Padé algorithm to efficiently solve range-dependent acoustic problems. RAM and RAMS assume that outgoing energy dominates over scattered energy, and compute the solution for the outgoing wave equation. An uncoupled azimuthal approximation is used to provide two-dimensional transmission loss values in range and depth. RAM has been enhanced by JASCO to approximately model shear wave conversion at the sea floor using the equivalent fluid complex density approach of Zhang & Tindle (1995). RAM is suitable when the top layer of seafloor can be modelled as a fluid, e.g. water-saturated sand or other unconsolidated sediment, and when shear-speeds are low. RAMS is suitable for acousto-elastic seafloors that can be modelled as a solid, e.g. rock, with high shear-speeds.

Because the modelling takes place over radial planes in range and depth, volume coverage is achieved by creating a fan of radials that is sufficiently dense to provide the desired tangential resolution. This $n \times 2D$ approach is modified in MONM to achieve greater computational efficiency by not over-sampling the region close to the source.

The desired coverage is obtained through a process of tessellation (Figure 8), whereby the initial fan of radials has a fairly wide angular spacing, but the arc length between adjacent radials is not allowed to increase beyond a pre-set limit before a new radial modelling segment is started, bisecting the existing ones. The new radial need not extend back to the source, because its starting acoustic field at the bisection radius is "seeded" from the corresponding range step of its neighbouring traverse.

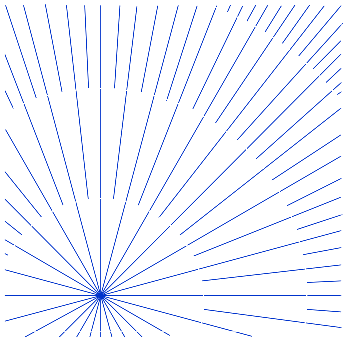

Figure 8: Sketch of tessellation; as the radial separation exceeds a pre-set limit, new fields are seeded.

The tessellation algorithm also allows the truncation of radials along the edges of a bounding quadrangle of arbitrary shape, further contributing to computational efficiency by enabling the modelling region to be more closely tailored to an area of relevance. MONM has the capability of modelling sound propagation from multiple directional sources at different locations and merging their acoustic fields into an overall received level at any given location and depth. This feature was not required in the present study, where only one pile driving operation was modelled.

Sound propagation modelling uses acoustic parameters appropriate for the specific geographic region of interest, including the expected water column sound speed profile, the bathymetry, and the bottom geoacoustic properties. MONM predicts the directional transmission loss as a function of depth and range from the source. The received level (*RL*) at any 3-dimensional location away from the source is calculated by combining the source level (*SL*) and transmission loss (*TL*), both of which are direction dependent, using the following equation:

$$RL = SL - TL$$

Acoustic transmission loss and received sound levels are a function of frequency, depth, range, bearing, and environmental properties. The received sound levels at any location within the region of interest are computed from the ⅓-octave band source levels by subtracting the numerically modelled transmission loss at each ⅓-octave band centre frequency, and summing incoherently across all frequencies to obtain a broadband value. The received levels estimated by MONM are equivalent to the sound exposure level (SEL) over the duration of a single source pulse. SEL is expressed in units of dB re $1\mu\text{Pa}^2 \cdot \text{s}$.

MONM requires the following environmental information.

3.2 Geology

Golder, in their geotechnical study of the TOT site (Golder 2007), cite a geological map by the Queensland Department of Mines indicating that the site is underlain by quaternary-age alluvium and colluvium sediments. Alluvium refers to sediments deposited by erosional processes (e.g. flowing streams and rivers); colluvium refers to rocks and soil accumulated at the foot of a slope by gravitational forces. These sediments rest on late-Palaeozoic-age granite rock.

Golder studied the sediment at the TOT site and undertook borehole measurements down to nearly 20m depth. They found ooze sediments at the top, down to about 1-3m depth. These included soft organic matter, as well as sand, silt and clay. Below the ooze, Golder found medium to dense sands and stiff to hard clay, down to 13-17m depth (Golder 2007). We were unable to find any measurements of seafloor geology below 20m. To the best of Golder's knowledge, deeper boreholes or geophysical velocity profiles have never been undertaken in the area (pers. comm. with Russel Jacobsen, 1 July 2008). Granite intrusions can be seen at nearby Castle Hill in Townsville, from which one can conclude that the bedrock will be granite. However, the depth of the granite and its geoacoustic properties are unknown.

For our sound propagation model, we used the following geoacoustic properties of the seafloor. We assumed a water-saturated sand-silt-clay mixture near the surface, decreasing in porosity and increasing in density and sound speed with depth. At 50m depth, we introduced a weathered granite bedrock, increasing in sound speed with depth as the granite becomes unweathered and denser. Geoacoustic properties and formulae for depth dependence were taken from Hamilton (1980), Thyssen (1980), and Orsi & Dunn (1991). MONM models sound propagation over the top 2000m of seafloor. At 2000m depth, attenuation is set high to account for energy lost into deeper depths.

Table 1: Geoacoustic properties of the seafloor.

Depth below seafloor [m]	**Density [g/cm^3]**	**Sound Speed [m/s]**	**Attenuation [dB/ λ]**	**Material**
0	1.59	1579	0.52	*Sand - silt - clay*
2	1.60	1581	0.51	
10	1.61	1591	0.49	
20	1.62	1604	0.46	
30	1.63	1617	0.44	
50	1.80	4500	0.09	*Granite*
1000	2.70	5500	0.13	
1900	2.75	6000	0.18	
2000	2.75	6000	10.00	

3.3 Seawater Properties

The properties of seawater in Cleveland Bay were studied by Walker (1981) and Wolanski *et al.* (1981). Samples from January were taken for our sound propagation model. The resulting sound speed profile is shown in the following figure.

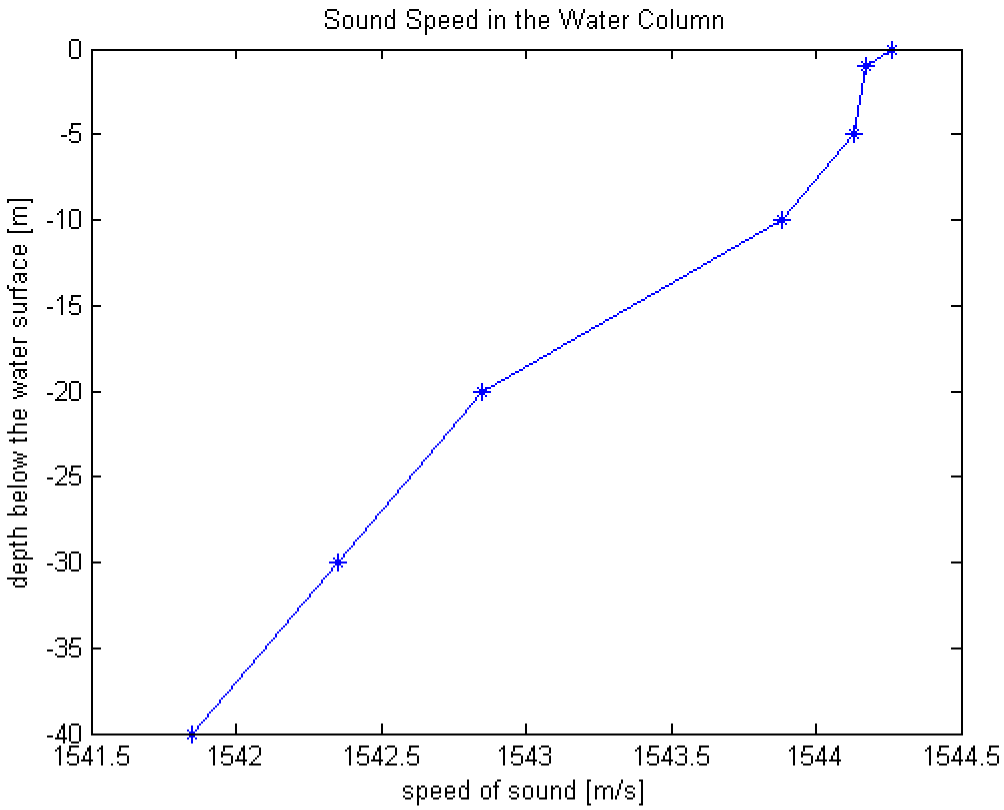

Figure 9: Sound speed in the water column taken from measurements in Cleveland Bay in January 1979.

3.4 Bathymetry

We digitized Chart AUS257 “Townsville Harbour and Ross River Entrance” of the Australian Hydrographic Service. The point 19°15’42’’S and 146°48’52’’E was chosen as our reference coordinate (0,0). Distances from this point were measured with a ruler, and depths were read off the chart. Distances were then converted to real ranges using the chart’s 1:7500 scale. Tide tables were obtained from Maritime Safety Queensland. We chose to model a high tide of 3.5m. Sound energy gets lost rapidly in shallow water. By modelling a high tide, we created a conservative scenario producing farther reaching sound contours.

Figure 10: Chart of Townsville Harbour.

Even though several 100m of sheet piles are proposed to be driven, we modelled only one pile in one particular location. The location was chosen conservatively, where sound propagation was expected to be best resulting in far-reaching sound contours. This location was chosen north-east of the end of the existing northern breakwater. Here, the water is deepest yielding best sound propagation characteristics. Also, this point is furthest from the existing breakwaters thus reducing the acoustic shielding effect by the breakwaters.

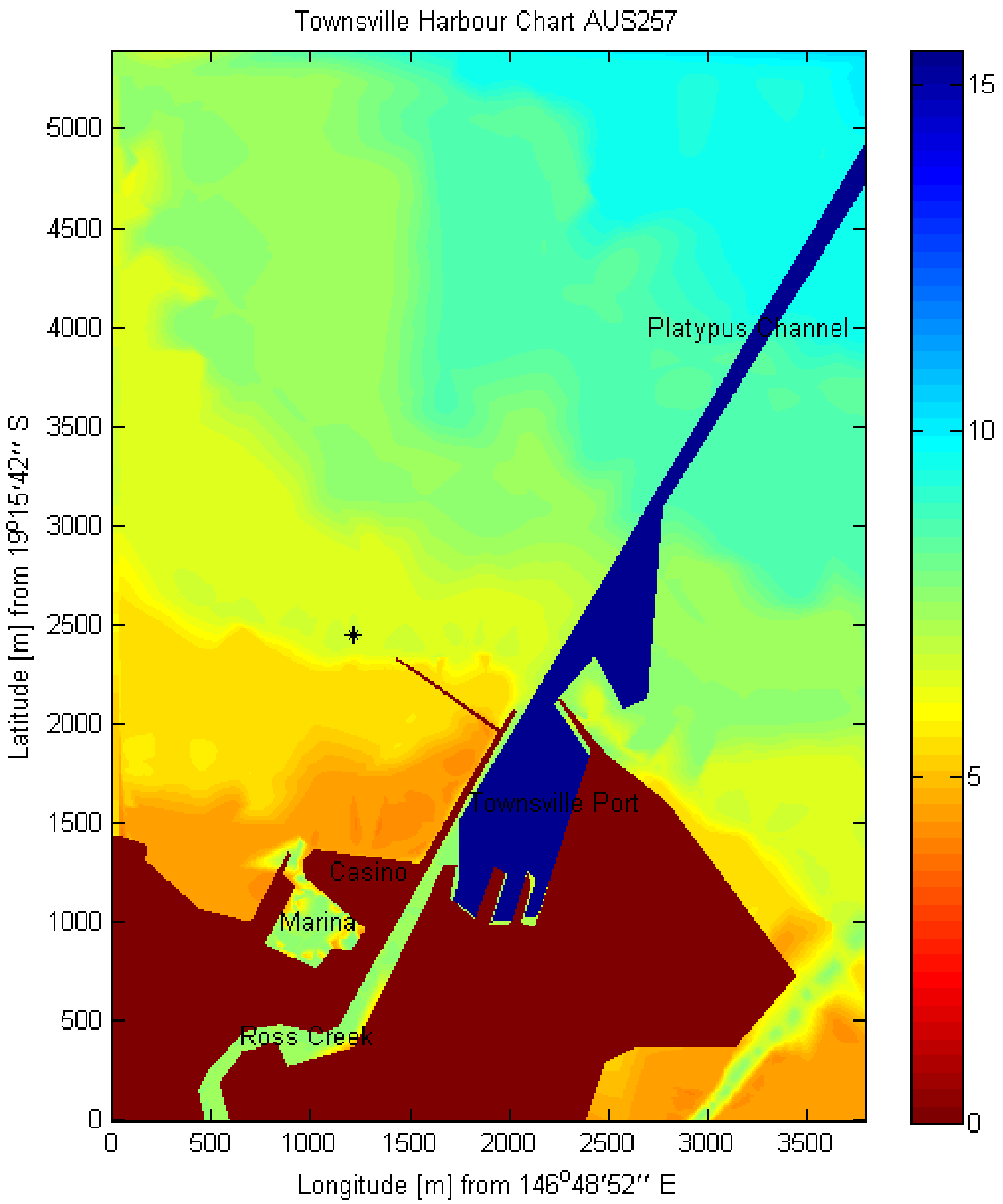

Figure 11: Digitized bathymetry. The bottom left corner is at 19°15'42''S and 146°48'52''E. The grid is in units of meters. Depths are indicated as colours [m]. A high tide of 3.5m above LAT is modelled. The dark blue area is the Platypus Channel going into the Port of Townsville, which is maintained at a depth of 11.7m below LAT. The brown area is land. The star indicates the pile driving location.

3.5 Results: Quiet Source

MONM was run for a quiet source with source spectrum levels corresponding to the lower envelope in Figure 7. For each longitude and latitude, the maximum received level over all depths was plotted in Figure 12. SEL are loudest at the source and drop as a function of range. The bathymetry affects the shape of the different SEL contours. The existing breakwaters provide some acoustic shielding. Sound levels are reduced inside the port and inside the marina south of the Casino. The sound received in the port, marina and Ross Creek travelled through the seafloor in our model. Received levels east of the Platypus Channel are also reduced, because the channel allows some sound energy to spread to deeper depths before being rapidly absorbed by the rising seafloor on the other side of the channel.

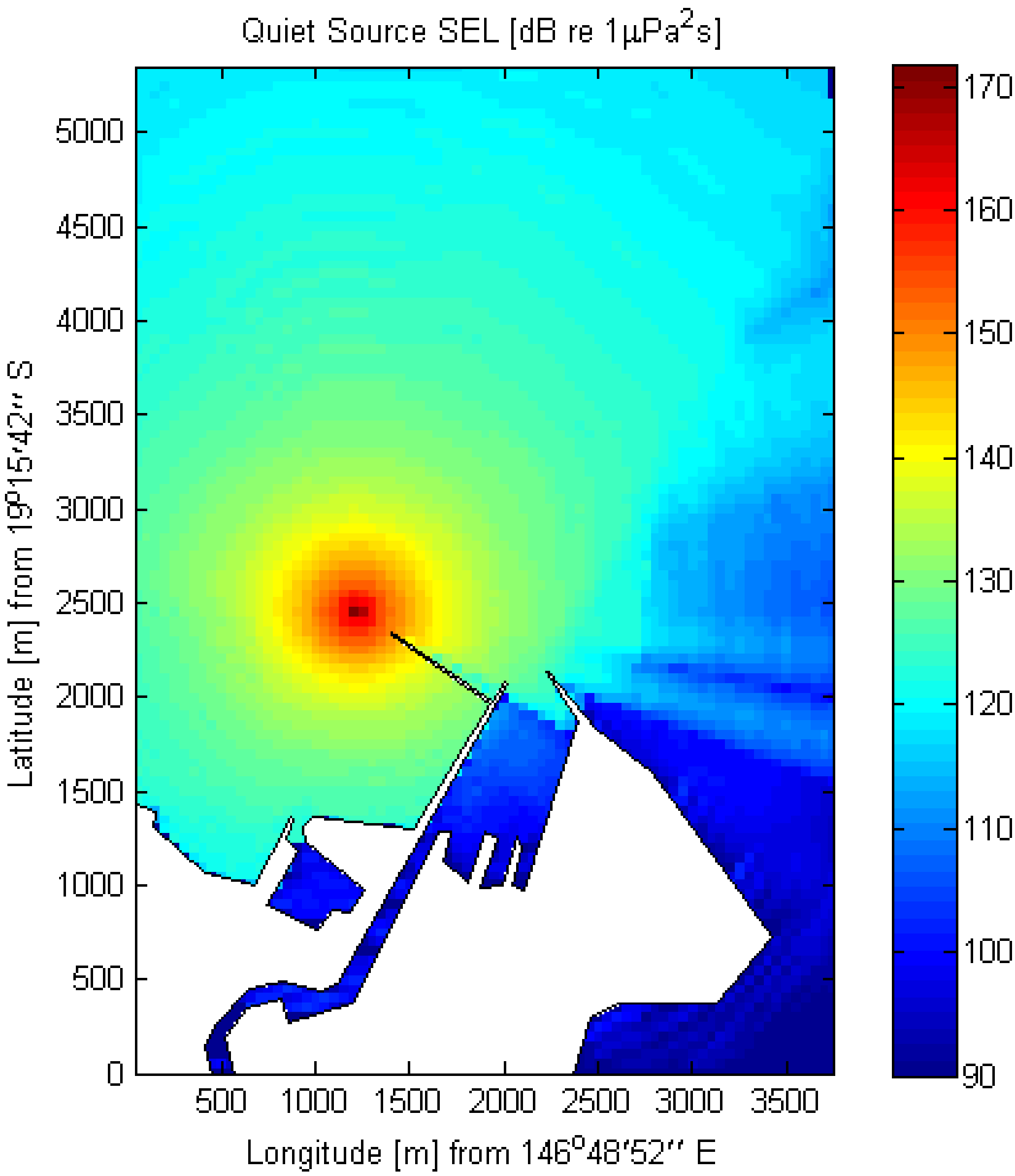

Figure 12: Received SEL from a quiet source. Plotted are the maximum SEL over all depths at each coordinate. Colours represent SEL in dB re 1µPa²s.

The following table lists some range measurements of a number of SEL contours.

Table 2: For the quiet source, this table describes the extent of the SEL contours. The maximum radius of the 170dB contour is 20m. The maximum extent of the 110dB contour is > 3.8km; the exact radius at this low level could not be determined, because the limits of the chart were reached. R95% gives the radius at which the sound is greater than the corresponding SEL for 95% of the time. E.g., over 2.5km range, the received level exceeds 120dB 95% of the time.

SEL Contour [dB re 1µPa^{2}s]	Rmax [km]	R95% [km]
110	> 3.815	> 3.098
120	2.790	2.522
130	1.023	0.941
140	0.456	0.441
150	0.214	0.205
160	0.059	0.059
170	0.020	0.020

3.6 Results: Loud Source

The sound propagation characteristics of the environment are, of course, independent of the source level. Therefore, the sound map for the loud source shows a similar pattern to the sound map of the quiet source. The breakwaters cause an acoustic shadow zone. The Platypus Channel reduces the amount of energy received in the water column on the eastern side of the channel. Sound gets absorbed fast over a rising seafloor, and travels further over a down-sloping seafloor. This is indicated by the density of SEL contours near the source. To the north of the source, SEL contours appear roughly circular. To the south, SEL contours are dented, as the water becomes shallower towards the shoreline.

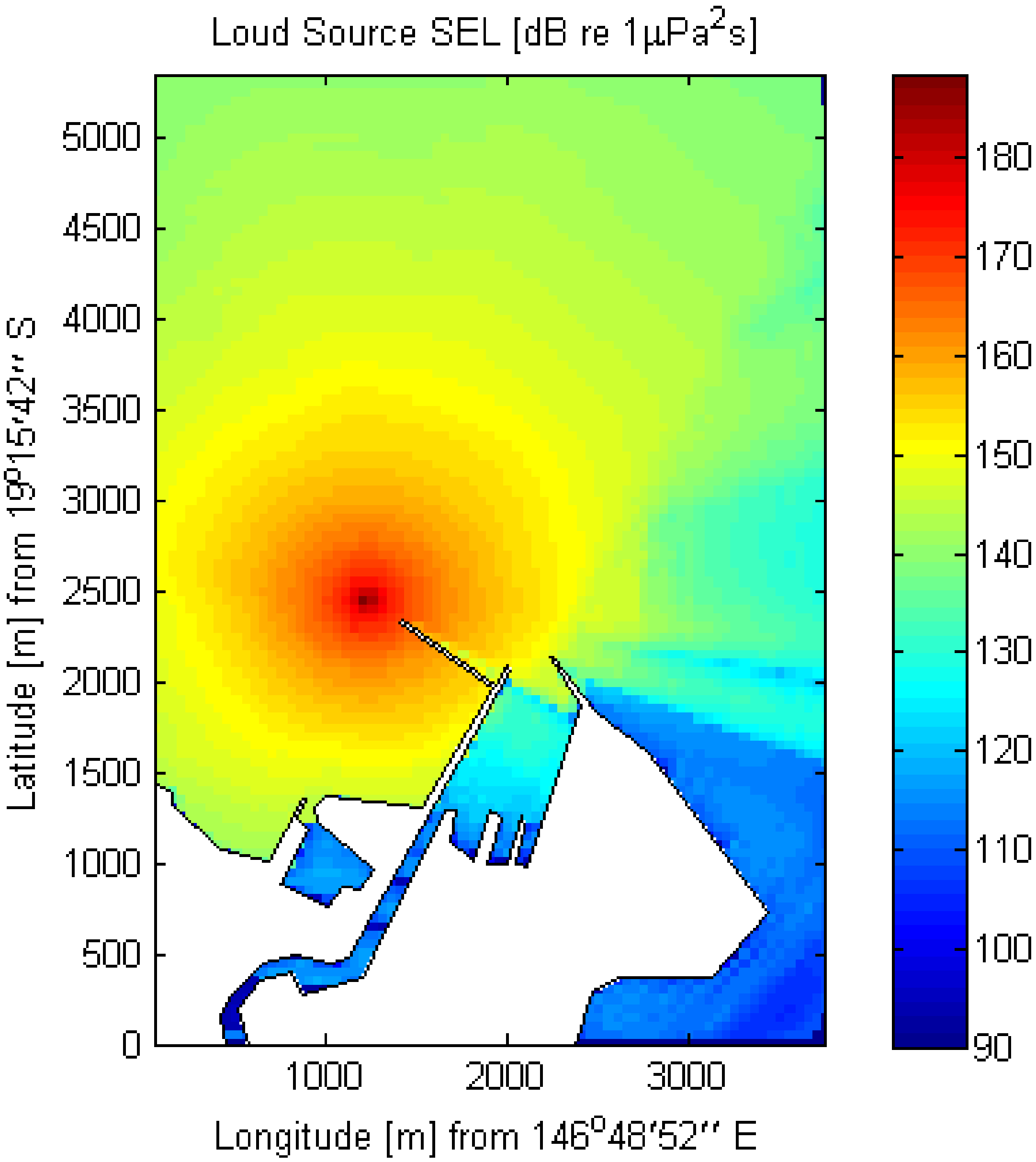

Figure 13: Received SEL from a loud source. Plotted are the maximum SEL over all depths at each coordinate. Colours represent SEL in dB re 1μPa²s.

The radii of a number of SEL contours are summarized in the following table. The ranges are longer than in the previous case of a quiet source. The full extent of the 130dB contour (and quieter contours) could not be determined, because the limits of the marine chart were reached. If model runs over longer ranges are desired, then this can be done using chart AUS256 "Cleveland Bay and Approaches" by the Australian Hydrographic Service.

Table 3: Extent of the different SEL contours for the loud source.

SEL Contour [dB re 1µPa^{2}s]	Rmax [km]	R95% [km]
130	> 3.815	> 3.093
140	3.307	2.924
150	1.310	1.217
160	0.522	0.499
170	0.191	0.186
180	0.030	0.030

4 Discussion

This study aimed to estimate underwater noise levels expected from pile driving operations at the Townsville Ocean Terminal site. As the size and shape of the piles, as well as the type and energy of the hammering mechanism, are still undecided, we reviewed the literature to produce an envelope of the potential source levels. We computed the minimum and maximum sound levels at each frequency from five different pile driving recordings, which we had access to. The minimum levels were used to model a quiet source at the TOT site; the maximum levels were used to model a loud source. JASCO's Marine Operations Noise Model computed transmission loss as a function of range, depth and azimuth, and produced sound maps for both sources.

We adopted a conservative approach to sound propagation modelling, in the sense that modelled levels will overestimate rather than underestimate real levels. The conservative choices we made are as follows. We chose to model a high tide of 3.5m, because sound gets absorbed very fast in shallow water. By choosing a high tide more sound energy will travel over longer ranges through the water column. Also, pile driving noise has most of its energy below 1kHz. Shallow water cannot support the propagation of low frequencies. The lower the tide, the faster the low frequencies will be attenuated. A high tide allows a broader sound spectrum to propagate.

We further chose the pile location conservatively. While several 100m of piles are planned to be driven, we had to pick one pile location for the model. This was chosen at the deeper end of the proposed development and at the corner farthest from the existing breakwaters to reduce sound shadowing.

In the absence of data on the acoustic properties of the existing breakwaters, these were simply modelled as raised seafloor, forcing the sound to propagate through the floor. If the acoustic properties of the breakwaters are close to those of the surrounding water, then the sound will go right through them, yielding higher levels than modelled. If the breakwater material is more absorptive than the seafloor, then they will produce lower sound levels on the other side than currently modelled. If the material is reflective, sound levels on the inside of the rectangle formed by the northern and port-western breakwaters and the casino will be louder.

Other uncertainties include the sound speed profiles in the water column and the seafloor. For the water column we used data from the 1970s. The growth of Townsville and its harbour over the past 30 years could likely have changed the water properties. However slight permanent changes as well as daily, monthly and seasonal fluctuations will likely have a small impact on the modelled sound maps. A larger impact has the uncertainty of the geoacoustic properties of the seafloor.

We strongly recommend underwater acoustic recordings during the early phases of pile driving in Townsville, in order to confirm or adjust the sound maps. If levels reach thresholds for marine animal impact, a choice of mitigation procedures exists. These include operational procedures (e.g. marine mammal detection and observation followed by shutting down if animals enter safety zones), or technological procedures (e.g. bubble screens).

5 References

Blackwell, S.B., J.W. Lawson and M.T. Williams. 2004. Tolerance by ringed seals (Phoca hispida) to impact pipe-driving and construction sounds at an oil production island. J. Acoust. Soc. Am. 115(5), 2346-2357.

Caltrans. 2001. Marine Mammal Impact Assessment: San Francisco – Oakland Bay Bridge East Span Seismic Safety Project; Pile Installation Demonstration Project.

Collins, M.D., R.J. Cederberg, D.B. King, and S.A. Chin-Bing. 1996. Comparison of algorithms for solving parabolic wave equations. J. Acoust. Soc. Am. 100(1), 178-182.

Golder Associates Pty Ltd. 2007. Townsville Ocean Terminal Project: Preliminary Geotechnical and Acid Sulphate Soils Investigation. Report to City Pacific Ltd.

Greene, C.R., S.B. Blackwell and M.W. McLennan. 2008. Sounds and vibrations in the frozen Beaufort Sea during gravel island construction. J. Acoust. Soc. Am. 123(2), 687-695.

Greeneridge Sciences and LGL. 1999. Piledriving and vessel sound measurements during installation of a gas production platform near Sable Island, Nova Scotia, during March and April 1998. Report for Sable Offshore Energy, Halifax NS, Canada.

Hamilton, E.L. 1980. Geoacoustic modelling of the sea floor. *J. Acoust. Soc. Am.* 68(5), 1313-1340.

JASCO. 2008. Modelling of Potential Underwater Noise from Pile Driving at the Townsville Ocean Terminal. Report for Applied Ecology Solutions. Brisbane, 20 June 2008.

Moulton, V.D., W.J. Richardson, M.T. Williams and S.B. Blackwell. 2003. Ringed seal densities and noise near an icebound artificial island with construction and drilling. Acoustics Research Letters Online 4(4), 112-117.

Nehls, G., K. Betke, S. Eckelmann and M. Ros. 2007. Assessment and costs of potential engineering solutions for the mitigation of the impacts of underwater noise arising from the construction of offshore windfarms. Cowrie Report ENG-01-2007.

Orsi, T.H., and D.A. Dunn. 1991. Correlations between sound velocity and related properties of glacio-marine sediments: Barents Sea. *Geo-Marine Letters* 11, 79-83.

Thyssen, F. 1980. Schallgeschwindigkeitsmessungen an Granit-Bohrkernen und Vulkanitstuecken. Measurements of the speed of sound in granite bore cores and volcanic rocks. *Geologisches Jahrbuch, Reihe A* 57, 126-129.

Walker, T. 1981. Seasonal salinity variations in Cleveland Bay, Northern Queensland. *Aust. J. Mar. Freshwater Res*. 32, 143-149.

Wolanski, E., M. Jones and W.T. Williams. 1981. Physical properties of Great Barrier Reef lagoon waters near Townsville. II Seasonal variations. *Aust. J. Mar. Freshwater Res.* 32, 321-334.